Paper No.
CMT25

Study of Hydrogen Embrittlement of API X65 & X80 Pipeline Steels using Short Fatigue Cracks

Dhiraj K. Mahajan
Indian Institute of Technology Ropar, Rupnagar-140001, India
dhiraj.mahajan@iitrpr.ac.in

Randhir Swarnkar, Yashpal Singh, Rajwinder Singh , Kanwer Singh Arora , Mahadev Shome, Gurmeet Singh

University of Delhi, Delhi-110007, India
Tata Steel Limited, Jamsedpur-831007, India,
Indian Institute of Technology Ropar, Rupnagar-140001, India

ABSTRACT

Hydrogen embrittlement can often lead to degradation of tensile strength, yield strength, ductility, fracture toughness as well as fatigue life of linepipe steel. API 5L X65 and API X80 steels are commonly used high strength linepipe steels, thus, understanding their hydrogen embrittlement behavior is of great interest. Extensive literature is available on long fatigue crack growth behavior of hydrogen charged API steels, using conventional CT specimens, that shows the effect of hydrogen embrittlement. However, it is the short fatigue crack growth behavior (microscopic cracks propagating through 8 to 10 grains) that can provide fundamental understanding and correlation of the steel microstructure with hydrogen embrittlement phenomenon. To this end, a new experimental framework is developed to investigate the short fatigue crack behavior of hydrogen charged API 5L X65 & X80 steels involving in-situ observation of propagating short cracks coupled with image processing to obtain da/dN vs Delta K curves.

Short fatigue crack growth behavior is characteristically different from long crack behavior showing high propagation rate as well as strong influence of microstructural barriers such as grain boundaries, phase boundaries and inclusions. Both the steels are compared for their short crack behavior after hydrogen charging and correlated with their hydrogen permeation behavior obtained using Devanathan-Stachurski cell thus giving detailed insight into the hydrogen embrittlement phenomenon observed for these steels.

Keywords: Hydrogen Embrittlement, API X80, API X65, Short fatigue cracks, Crack propagation

INTRODUCTION

Hydrogen is being considered as a future energy carrier that can significantly reduce air pollution currently being caused by the fossil fuels. Among various form of stored hydrogen, compressed gaseous hydrogen has emerged as the most feasible solution for both mobile (e.g. automobiles) and stationary (e.g. telecom towers) hydrogen based energy applications. Thus, for future hydrogen based economy, it is essential to develop safe, conformable, cost effective gaseous hydrogen transportation systems. For this reason, it is considered to use the existing API 5L steel pipeline network currently being used for the natural gas transportation for the transportation of high pressure gaseous hydrogen[1–3]. However, these metallic pipelines are prone to embrittlement (loss of mechanical properties) under the influence of hydrogen, a property often called as Hydrogen Embrittlement (HE). Hydrogen embrittlement is a phenomenon that generally leads to degradation of tensile strength, yield strength, ductility, fracture toughness as well as fatigue life of steels. Therefore, to design a safer and reliable hydrogen transport infrastructure, it is essential to develop a micro-structural and metallurgical basis of HE for determining the propensity of different pipeline steels to failure under high pressure gaseous hydrogen environment.

API 5L X65 and API X80 steels are commonly used high strength linepipe steels, thus, understanding their hydrogen embrittlement behavior is of great interest. Extensive characterization of these steels using static loads under high-pressure hydrogen service environment have shown variation in their hydrogen embrittlement susceptibility depending upon the microstructural features[4,5]. Stress-controlled fatigue-life studies on these steels in the presence of high-pressure hydrogen has also emphasized a quantifiable decrease[6]. Understanding the fatigue behavior of these steels under hydrogen environments is important due to its relevance in high pressure system components. Such understanding can lead to the optimized selection of API steel with enhanced safety and reduced cost of the hydrogen handling pipeline infrastructure[7].

Total fatigue life of a component can be divided into fatigue crack initiation and fatigue crack growth phase, in which fatigue crack initiation contribution can be up to 90% of the total fatigue life. Fatigue crack initiation is linked with the short fatigue crack propagations as shown in Figure 1, the size of which is of the order of grain size (few hundred microns), and are generally not detectable by conventional crack detection techniques (DC Potential Drop: DCPD, Digital Image Correlation: DIC). Short fatigue crack growth behavior is characteristically different from long crack behavior showing high propagation rate as well as strong influence of microstructural barriers such as grain boundaries, phase boundaries and inclusions. Understanding the short fatigue crack growth behavior in steels under hydrogen environments can link the microscopic origin of fatigue cracks with their microstructural features (such as phase/grain boundaries, grain orientation).

Understanding the microscopic origin of short cracks will consequently help to improve the selection of materials and microstructures with improved fatigue life under hydrogen environments. To this end, a new experimental framework is developed to investigate the short fatigue crack behavior of hydrogen charged API 5L X65 & X80 steels involving in-situ observation of propagating short cracks coupled with image processing to obtain $\frac{da}{dN}\ vs\ \Delta K$ curves. Both the steels are compared for their short crack behavior after hydrogen charging and correlated with their hydrogen permeation behavior obtained using Devanathan-Stachurski cell thus giving detailed insight into the hydrogen embrittlement phenomenon observed for these steels.

This paper consists of four sections. Following this brief introduction, section 2 describes the materials used for investigations, test devices and procedures. Section 3 presents the results obtained which is followed by conclusions.

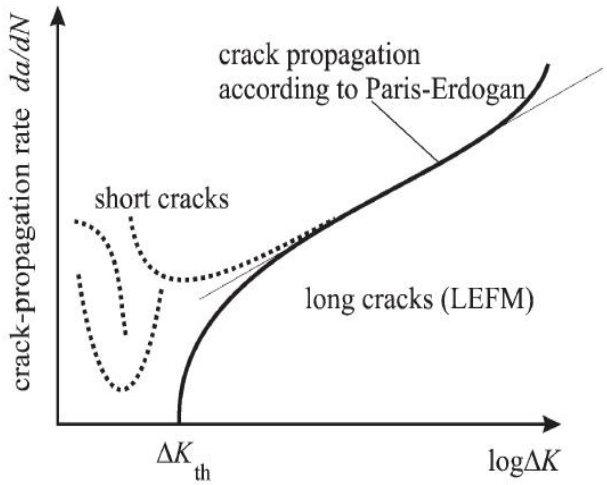

Figure 1: Characteristics of short fatigue crack propagation showing high crack growth rate below the threshold stress intensity factor range (ΔK_{th}) obtained from long crack behavior.

EXPERIMENTAL PROCEDURE

The chemical composition of API X65 and API X80 pipeline steel is given in Table 1 and 2 respectively. The optical micrographs of both steels at 500X magnification is shown in Figure 2 showing smaller grain size for API X80. The microstructure for API X65 steel samples has been confirmed to be of banded ferrite-pearlite type while API X80 samples has acicular ferrite type microstructure.

Table 1: Chemical composition of API 5L X65 steel

C(%)	Mn(%)	S(%)	P(%)	Si(%)	Al(%)	N(ppm)	V(%)	Nb(%)	Mo(%)
0.0541	1.498	0.0011	0.0121	0.2302	0.0288	54	0.0355	0.0572	0.086

Table 2: Chemical composition of API 5L X80 steel

C(%)	Mn(%)	S(%)	P(%)	Si(%)	Cr(%)	Cu(%)	V(%)	Nb(%)	Mo(%)	Ni (%)
0.04	1.8	0.001	0.012	0.24	0.05	0.18	0.018	0.483	0.18	0.19

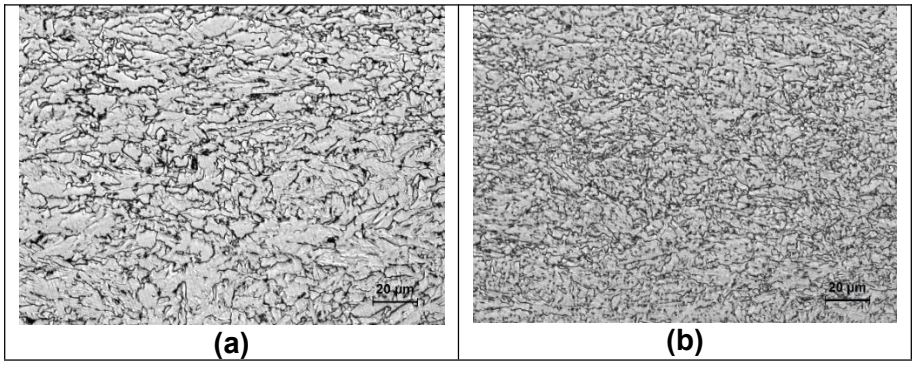

Figure 2: Optical micrograph of (a) API X65 (b) API X80 at 500X

Hydrogen Permeation Experiments

An In-house fabricated Devanathan-Stachurski permeation cell is used for the characterization of hydrogen permeation behavior of both the steels using dual channel electrochemical workstation having common working electrode as the metal specimen and two sets of counter and reference electrodes for the galvanostatic and the potentiostatic of the cell[8]. The cell in the disassembled configuration in shown in Figure 3. Circular specimens of both the steels with 10 mm diameter and 1 mm thickness is used after grinding and polishing the surface for permeation studies. Permeation current is measured with time until steady state is reached and effective diffusion coefficient is deduced according to equation:

$$j_\infty = \frac{FD}{L} C_s \qquad \rightarrow (1)$$

where j_∞ (mol·mm^{-1}·s^{-1}) is hydrogen flux; D (mm^2·s^{-1}) is effective diffusion coefficient which is determined for both steels; C_s (mol·mm^{-3}) is the concentration at which H+ ions are generated in the electrolyte on the cathodic side, *L* (mm) is the thickness of the specimen and *F* is Faraday's constant.

Figure 3: An In-house fabricated Devanathan-Stachurski cell shown in the disassembled configuration. Among the three compartments shown, the middle one holds the metal specimen exposing both its surfaces to the electrolyte in the right and left compartments those being the galvanostatic and the potentiostatic side of the cell.

Cathodic Hydrogen Charging of Metal Specimens

For hydrogen embrittlement testing, tensile and fatigue specimens are charged with hydrogen using electrochemical method by exposing the specimen to electrolyte containing 0.1N H_2SO_4 + 1.4 g/mL thiourea (charging promotor) under current density of 40 mA/cm^2 for 4 hours. Platinum mesh is used as anode for hydrogen charging.

Tensile and Fatigue Testing of Metal Specimens

Tensile and fatigue tests are performed on 5 mm thick samples having dimensions as shown in Figure 4 in the uncharged and hydrogen charged state. For short fatigue crack propagation studies, a sharp notch in the fatigue samples is generated using precision laser cutting on a micro-machining center. Crack thus generated has approximately 100 µm width and 1 mm initial length. Side view of the fatigue specimens is shown in Figure 5. Fatigue crack propagation studies are performed at 20 Hz while a sharp initial crack is obtained from the notch using higher frequency fatigue loading.

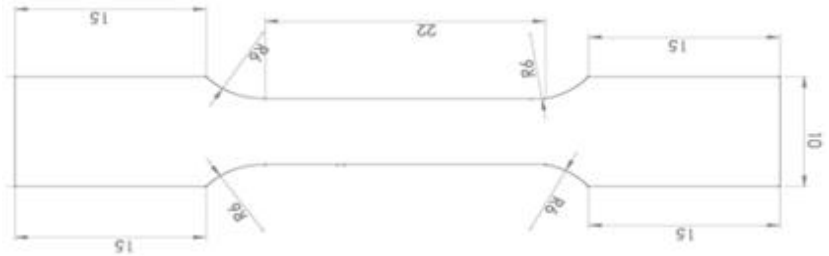

Figure 4: Dimensions (in mm) of tensile and fatigue specimens

Figure 5: Side view of the fatigue specimen used for short fatigue crack studies. A sharp crack is generated on one edge of the specimens using precision laser cutting on a micro-machining center. Crack thus generated has approximately 100 µm width and 1 mm initial length.

In-Situ Tracking of Short Fatigue Crack

Two high resolution digital microscopes are used for in-situ tracking of the propagating short fatigue cracks. While one microscope with maximum magnification of 200X is permanently with the fatigue machine in vertical configuration (as shown in Figure 6) to monitor the propagating crack, the second microscope with maximum magnification of 800X is used in horizontal configuration for taking high resolution micrographs at cyclic intervals of interest to determine increase in the crack length using ImageJ software[9] based image processing.

Figure 6: High resolution digital microscopes used for tracking the propagating short fatigue crack

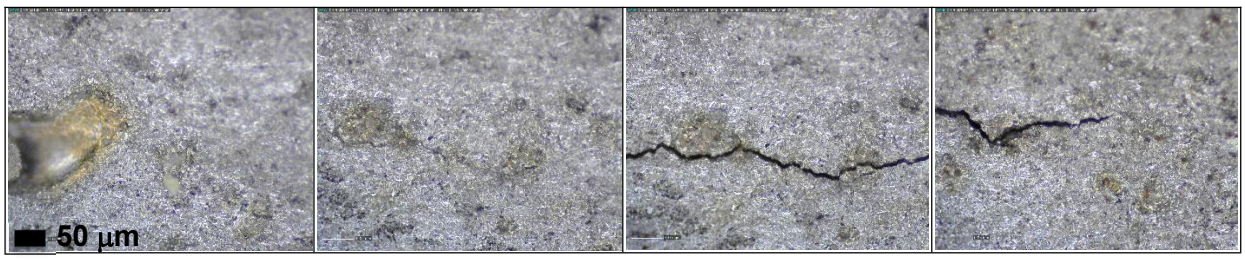

Figure 7: A propagating short fatigue crack with increasing number of cycles (from left to right) originated from the crack tip (left). Pictures are obtained using high resolution digital microscope with maximum magnification of 800X. The length bar shown in the black color is of 50 µm length.

Results

Hydrogen Permeation Behavior

Based on equation (1), the obtained value of effective diffusion coefficient (*D*) of API X80 and API X65 from permeation experiments is 1.32×10^{-9} m^2/s and 1.15×10^{-9} m^2/s respectively. The data obtained from permeation experiments in given in Figure 8. It shows that API X80 steel can permeate hydrogen 1.15 times more compared to API X65 steel. The effective diffusion coefficient consists of both the lattice as well as trapped hydrogen contribution showing that microstructural features of API X65 have more trapping sites compared to API X80 even though the latter has finer grains. Due to lower value of *D,* it is expected that API X65 can be more prone to hydrogen embrittlement.

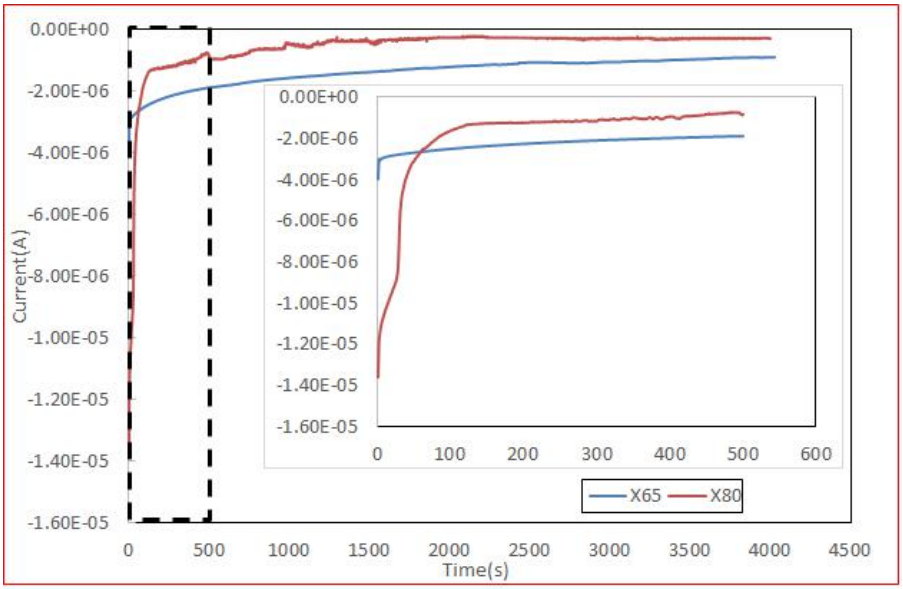

Figure 8: Permeation transient comparison of API X80 and API X65 specimens

Effect of Hydrogen on Uniaxial Deformation Behavior

Comparison of tensile behavior of both the steels in uncharged and charged state is shown in Table 3. Hydrogen leads to more deterioration in the tensile properties of API X65 steels compared to API X80, as expected from permeation experiments.

Table 3: Effect of hydrogen on tensile behavior of API X65 and API X80 specimens

Specimen	Yield Strength(MPa)	Ultimate Strength(MPa)	Elongation at fracture (%)
X65, uncharged	570	630	41
X65, hydrogen charged (40mA/cm^2, 4 hours)	530	597	30
X80, uncharged	612	724	43
X80, hydrogen charged (40mA/cm^2, 4 hours)	580	702.5	36

Effect of Hydrogen on Short Fatigue Crack Propagation Behavior

Short fatigue crack propagation behavior for API X65 and API X80 in charged and uncharged state is shown in Figure 9. In this plot, the number of cycles from which increase in the initial crack length is tracked is set to zero for ease in comparison of the data obtained for all four specimens. The presence of hydrogen leads to sharp increases in the short fatigue crack length for API X65 steel compared to API X80 in-line with the expectations from the permeation behavior.

A combined plot of $\frac{da}{dN}$ vs ΔK behavior for all four specimens is shown in Figure 10. The valleys in these plots specially represents the microstructural features such as grain or phase boundary that provide a hindrance for the propagation of short fatigue crack. In general, the hydrogen charged specimen showed high crack growth rate and lesser hindrances for the short crack propagation. Compared to API X80, hydrogen effects API X65 more severely as expected from their hydrogen permeation behavior.

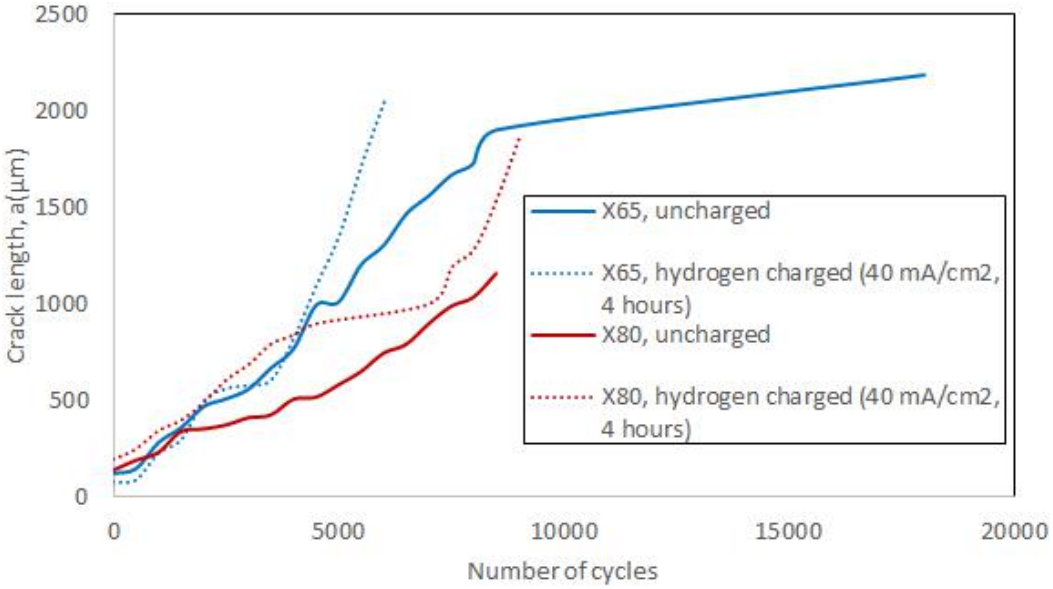

Figure 9: Variation of short fatigue crack length vs number of cycles for API X65 and API X80 steel specimens in hydrogen charged and uncharged state. The number of cycles from which the increase in the initial crack length is tracked is set to zero for ease in comparison.

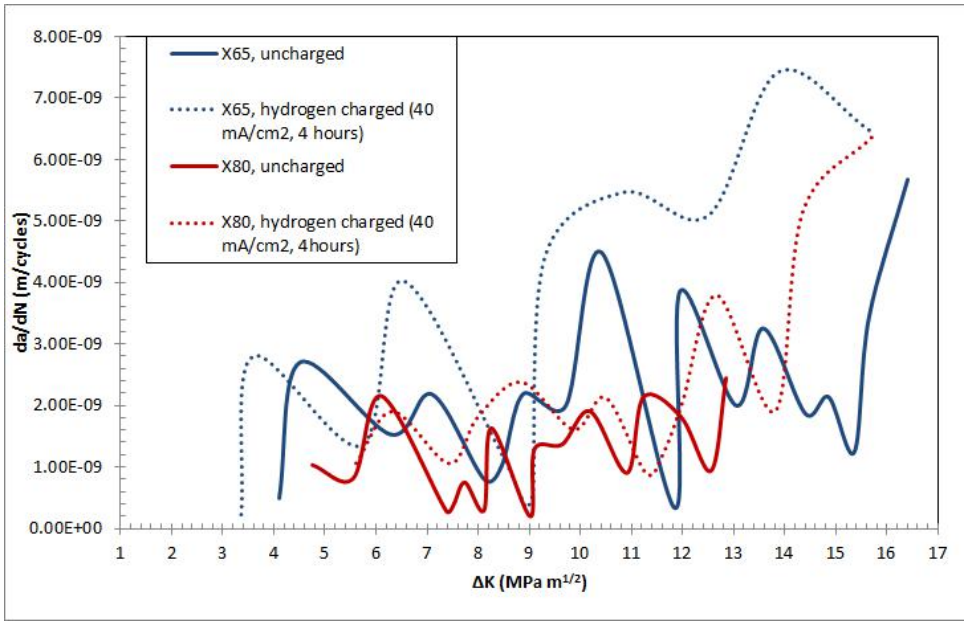

Figure 10: The effect of hydrogen on $\frac{da}{dN}$ vs ΔK behavior shows higher crack growth rate for hydrogen charged specimens in addition to lesser resistance to crack propagation due to microstructural features such as grain or phase boundaries.

CONCLUSIONS

An experimental framework is presented to study the Hydrogen Embrittlement phenomenon in API X65 & API X80 linepipe steels using short fatigue cracks. It involves in-situ observation of propagating short fatigue cracks coupled with image processing to obtain their $\frac{da}{dN}$ vs ΔK curves. Though variation in their short fatigue crack propagation behavior confirms hydrogen embrittlement phenomena, it is still cumbersome process to link it with the microstructural features of both API X65 and API X80 steels. The limitation of the framework is rendered by the maximum magnification of the digital microscopes used in this work as it limits the size of smallest crack that can be tracked using this framework.

The hydrogen permeation behavior obtained for both the steels correlated well with their hydrogen embrittlement behavior that shows API X65 steel to be much severely affected by hydrogen compared API X80. API X80 steel even through has small grain size compared to API X65, it is the difference in their microstructural features that lead to different mechanisms of hydrogen trapping and thus different level of damage due to hydrogen embrittlement[10].

Future work will focus on more detailed study of hydrogen embrittlement phenomenon using short fatigue crack behavior of these two steels obtained using newly installed fatigue stage for FESEM coupled with their EBSD data.

References

1. Briottet, L., Batisse, R., Dinechin, G. de, Langlois, P. & Thiers, L. Recommendations on X80 steel for the design of hydrogen gas transmission pipelines. *International Journal of Hydrogen Energy* **37,** 9423–9430 (2012).
2. American Petroleum Institute. API 5L: Specification for Line Pipe.
3. Ningileri, S. T., Boggess, T. A. & Stalheim, D. Materials Solutions for Hydrogen Delivery in Pipelines (2013).
4. Moro, I. *et al.* Hydrogen embrittlement susceptibility of a high strength steel X80. *Materials Science and Engineering: A* **527,** 7252–7260 (2010).
5. Stalheim, D. *et al. in Proceedings of the ASME international pipeline conference 2010* (American Society of Mechanical Engineers, New York, N.Y., 2010), pp. 529–537.
6. An, T. *et al.* Synergistic action of hydrogen and stress concentration on the fatigue properties of X80 pipeline steel. *Materials Science and Engineering: A* **700,** 321–330 (2017).
7. San Marchi, C. & Somerday, B. P. in *Proceedings of the ASME pressure vessels and piping conference, 2014,* edited by C. San Marchi & B. P. Somerday (ASME2014), V06BT06A023.
8. ASTM. Practice for Evaluation of Hydrogen Uptake, Permeation, and Transport in Metals by an Electrochemical Technique.
9. Schneider, C. A., Rasband, W. S. & Eliceiri, K. W. NIH Image to ImageJ. 25 years of image analysis. *Nat Meth* **9,** 671–675 (2012).
10. Tovee & John-Paul. Microstructural influence on the effects of forward and reverse mechanical deformation in HSLA X65 and X80 linepipe steels. Available at http://etheses.bham.ac.uk/5171/ (2014).